SUSY at the LHC

Yeong Gyun Kim[1]

ARCSEC, Sejong University, Seoul 143-747, Korea
Department of Physics, KAIST, Daejon 305-017, Korea

Abstract

We consider a few selected topics on SUSY phenomenology at the LHC. The signatures of mirage mediation at the LHC is discussed. The τ polarization effects on SUSY cascade decay is presented. A new collider observable 'gluino m_{T2}' is introduced and its physical property is investigated.

1 Introduction

The Large Hadron Collider (LHC) at CERN will soon explore TeV energy scale, where new physics beyond the Standard Model (SM) is likely to reveal itself [1, 2]. Among various proposals, weak scale supersymmetry (SUSY) is perhaps the most promising candidates of new physics beyond the standard model (SM) [3]. It provides a solution for gauge hierarchy problem and complies with gauge coupling unification. Another nice feature of the SUSY theory with R-parity conservation is that the lightest supersymmetric particle (LSP) is a natural candidate for the non-baryonic dark matter (DM) in the universe.

SUSY phenomenology crucially depends on SUSY particle masses and other physical properties, which might result from spontaneous SUSY breaking in a hidden sector. The SUSY breaking is communicated to visible sector through some messenger interactions depending on models. Soft SUSY breaking terms of visible matter fields are then determined such that different SUSY breaking and mediating mechanism leads to different pattern of masses and properties of SUSY particles.

Once SUSY signals are discovered through event excess beyond the SM backgrounds in inclusive search channels, the next step will be the measurements of SUSY particle masses and other physical properties in various exclusive decay chains. Then it might be possible to reconstruct SUSY theory, in particular SUSY breaking mechanism from the experimental information on SUSY particle masses. In this regard, determination of gaugino masses has a significant implication because predictions of the gaugino masses are rather robust compared to those on sfermion masses [4].

Here, we consider a few selected topics on SUSY phenomenology at the LHC. In section 2, we investigate the LHC signatures of the mirage mediation performing a Monte Carlo study for a benchmark point in the scenario and show that SUSY particle masses can be determined in a model independent way, providing some valuable information on SUSY breaking sector [5].

In section 3, τ polarization effects in SUSY cascade decay is investigated [6]. The τ leptons emitted in cascade decays of supersymmetric particles are polarized. The polarization may be exploited to determine spin and mixing properties of the neutralinos and stau particles involved.

Finally, in section 4, we introduce a new observable, 'gluino m_{T2}' [7], which is an application of the Cambridge m_{T2} variable to the process where gluinos are pair produced in proton-proton collision and each gluino subsequently decays into two quarks and one LSP, *i.e.* $\tilde{g}\tilde{g} \to qq\tilde{\chi}_1^0\, qq\tilde{\chi}_1^0$. We show that the gluino m_{T2} can be utilized to measure the gluino and the lightest neutralino masses separately, and also the (1st and 2nd generation) squark masses if lighter than the gluino mass, thereby providing a good first look at the pattern of sparticle masses experimentally.

[1]ygkim@muon.kaist.ac.kr

2 LHC signatures of Mirage mediation

Kachru *et al.* (KKLT) has provided a concrete set-up of string compactification, in which all moduli are fixed and Minkowski (or de Sitter) vacuum is achieved [8]. The KKLT-type moduli stabilization scenario leads to an interesting pattern of soft SUSY breaking terms, to which modulus and anomaly contributions are comparable to each other if gravitino mass $m_{3/2} \sim 10$ TeV [9]. A noticeable feature of the mixed modulus-anomaly mediation (*a.k.a* mirage mediation) is that soft masses are unified at a mirage messenger scale [10]

$$M_{mir} = M_{GUT} \left(\frac{m_{3/2}}{M_{Pl}} \right)^{\alpha/2} \tag{1}$$

with α representing the ratio of the anomaly to modulus mediation. The mirage messenger scale M_{mir} is hierarchically lower than M_{GUT} for a positive $\alpha \sim O(1)$. Such a low (mirage) unification scale for soft masses leads to a SUSY mass spectrum which is quite distinctive from those in other SUSY breaking scenarios such as mSUGRA, gauge mediation and anomaly mediation. Some phenomenological aspects of the mirage mediation have been investigated by several authors [11, 12].

If the weak scale SUSY is realized in nature, SUSY particles would be produced copiously at the LHC [13, 14], which is scheduled to start in 2008. Gluinos and squarks, which are directly produced from the proton-proton collision, will decay to the LSP and SM particles in the end, with non-colored SUSY particles as intermediate states in general. The precise measurement of the masses of SUSY particles might be possible with reconstruction of the cascade decay chains [15, 16]. Kinematic edges and thresholds of various invariant mass distributions can be measured experimentally and then the SUSY particle masses would be determined in a model independent way. In turn, SUSY breaking mechanism might be reconstructed from the measured SUSY spectrum and signatures.

2.1 Mirage Mediation

In KKLT-type moduli stabilization scenario, the light modulus T which determines the SM gauge couplings is stabilized by non-perturbative effects and the SUSY-breaking source is sequestered from the visible sector. The non-perturbative stabilization of T by modulus superpotential results in a suppression of the modulus F component:

$$\frac{F^T}{T} \sim \frac{m_{3/2}}{\ln(M_{Pl}/m_{3/2})}, \tag{2}$$

which is comparable to anomaly mediated soft mass of $O(m_{3/2}/4\pi^2)$ for $m_{3/2}$ near the TeV scale. The soft terms of visible fields are then determined by the modulus mediation and the anomaly mediation if the SUSY breaking brane is sequestered from the visible sector. The soft terms of canonically normalized visible fields are given by

$$\mathcal{L}_{\rm soft} = -\frac{1}{2} M_a \lambda^a \lambda^a - \frac{1}{2} m_i^2 |\phi_i|^2 - \frac{1}{6} A_{ijk} y_{ijk} \phi_i \phi_j \phi_k + \text{h.c.}, \tag{3}$$

where λ^a are gauginos, ϕ_i are the scalar component of visible matter superfields $_i$ and y_{ijk} are the canonically normalized Yukawa couplings. For $F^T/T \sim m_{3/2}/4\pi^2$, the soft parameters at energy scale just below M_{GUT} are determined by the modulus-mediated and anomaly-mediated contributions which are comparable to each other. One then finds the boundary values of

gaugino masses, trilinear couplings and sfermion masses at M_{GUT} are given by

$$\begin{aligned} M_a &= M_0\Big[1+\frac{\ln(M_{Pl}/m_{3/2})}{16\pi^2}b_a g_a^2\alpha\Big], \\ A_{ijk} &= M_0\Big[(a_i+a_j+a_k)-\frac{\ln(M_{Pl}/m_{3/2})}{16\pi^2}(\gamma_i+\gamma_j+\gamma_k)\alpha\Big], \\ m_i^2 &= M_0^2\Big[c_i-\frac{\ln(M_{Pl}/m_{3/2})}{16\pi^2}\theta_i\alpha-\left(\frac{\ln(M_{Pl}/m_{3/2})}{16\pi^2}\right)^2\dot{\gamma}_i\alpha^2\Big], \end{aligned} \tag{4}$$

where α represents the anomaly to modulus mediation ratio:

$$\alpha \equiv \frac{m_{3/2}}{M_0\,\ln(M_{\rm Pl}/m_{3/2})}\,, \tag{5}$$

with M_0 the pure modulus mediated gaugino mass, while a_i and c_i parameterize the pattern of the pure modulus mediated soft masses. The one-loop beta function coefficient b_a, the anomalous dimension γ_i and its derivative $\dot{\gamma}_i$ and θ_i are defined by

$$\begin{aligned} b_a &= -3\mathrm{tr}\ T_a^2(\mathrm{Adj}) + \sum_i \mathrm{tr}\ T_a^2(\phi_i)\ , \\ \gamma_i &= 2\sum_a g_a^2 C_2^a(\phi_i) - \frac{1}{2}\sum_{jk}|y_{ijk}|^2, \\ \dot{\gamma}_i &= 8\pi^2\frac{d\gamma_i}{d\ln\mu}, \\ \theta_i &= 4\sum_a g_a^2 C_2^a(\phi_i) - \sum_{jk}|y_{ijk}|^2(a_i+a_j+a_k), \end{aligned} \tag{6}$$

where the quadratic Casimir $C_2^a(\phi_i)=(N^2-1)/2N$ for a fundamental representation ϕ_i of the gauge group $SU(N)$, $C_2^a(\phi_i)=q_i^2$ for the $U(1)$ charge q_i of ϕ_i, and $\omega_{ij}=\sum_{kl}y_{ikl}y^*_{jkl}$ is assumed to be diagonal. In this prescription, generic mirage mediation is parameterized by

$$\alpha,\ M_0,\ a_i,\ c_i,\ \tan\beta, \tag{7}$$

where $\tan\beta$ is the ratio of the vacuum expectation values of the two neutral Higgs fields.

An interesting feature called mirage mediation arises from the soft masses of Eq. (4) at M_{GUT}, due to the correlation between the anomaly mediation and the RG evolution of soft parameters. The low energy gaugino masses are given by [10]

$$M_a(\mu) = M_0\left[1-\frac{1}{8\pi^2}b_a g_a^2(\mu)\ln\left(\frac{M_{\rm mir}}{\mu}\right)\right] = \frac{g_a^2(\mu)}{g_a^2(M_{\rm mir})}M_0, \tag{8}$$

implying that the gaugino masses are unified at $M_{\rm mir}$, while the gauge couplings are unified at M_{GUT}. If the y_{ijk} is small or $a_i+a_j+a_k=c_i+c_j+c_k=1$, the low energy values of A_{ijk} and m_i^2 are given by [10]

$$\begin{aligned} A_{ijk}(\mu) &= M_0\left[a_i+a_j+a_k+\frac{1}{8\pi^2}(\gamma_i(\mu)+\gamma_j(\mu)+\gamma_k(\mu))\ln\left(\frac{M_{\rm mir}}{\mu}\right)\right], \\ m_i^2(\mu) &= M_0^2\left[c_i-\frac{1}{8\pi^2}Y_i\left(\sum_j c_j Y_j\right)g_Y^2(\mu)\ln\left(\frac{M_{GUT}}{\mu}\right)\right. \\ &+ \left.\frac{1}{4\pi^2}\left\{\gamma_i(\mu)-\frac{1}{2}\frac{d\gamma_i(\mu)}{d\ln\mu}\ln\left(\frac{M_{\rm mir}}{\mu}\right)\right\}\ln\left(\frac{M_{\rm mir}}{\mu}\right)\right], \end{aligned} \tag{9}$$

where Y_i is the $U(1)_Y$ charge of ϕ_i. Therefore, the first- and second-generation sfermion masses are also unified at the M_{mir} scale if the modulus-mediated squark and slepton masses have a common value, i.e. $c_{\tilde{q}} = c_{\tilde{\ell}}$ ($\equiv c_M$).

Phenomenology of mirage mediation is quite sensitive to the anomaly to modulus mediation ratio α as well as the parameters a_i and c_i [10, 11, 12]. When α increases from zero to a positive value of order unity, the nature of the neutralino LSP is changed from bino-like to Higgsino-like via a bino-Higgsino mixing region. This feature can be understood from the dependence of the gaugino masses on α. The gluino mass M_3 decreases as α increases, while the bino mass M_1 increases. Smaller M_3 then leads to smaller $|m_{H_u}^2|$ and Higgsino mass parameter $|\mu|$ at the weak scale through smaller stop mass square. While the gaugino masses are not sensitive to a_i and c_i, the low energy squark, slepton and Higgs masses depend on those parameters through their boundary values at M_{GUT} and their RG evolutions and the mass mixing induced by the low energy A parameters.

For the original KKLT compactification of type IIB string theory [8], one finds that $\alpha = 1$, $a_i = c_i = 1 - n_i$, where n_i are modular weights of the visible sector matter fields depending on the origin of the matter fields. The corresponding mirage messenger scale for $\alpha = 1$ is given by $M_{mir} \sim 3 \times 10^9$ GeV. Such an intermediate (mirage) unification scale which is hierarchically smaller than M_{GUT}, leads to quite a degenerated sparticle mass spectrum at EW scale, compared to that for mSUGRA-type pure modulus mediation ($\alpha = 0$). Here, we will consider the intermediate scale mirage mediation ($\alpha = 1$) as a benchmark scenario for a detailed Monte Carlo study of LHC phenomenology.

2.2 Collider signatures

2.2.1 A benchmark point

We perform a Monte Carlo study for LHC signatures of mirage mediation with the following model parameters;

$$\alpha = 1,\ M_0 = 500\ \text{GeV},\ a_M = c_M = 1/2,\ a_H = c_H = 0,\ \tan\beta = 10, \tag{10}$$

where c_M is a common parameter which parameterize the pattern of the pure modulus mediated masses for squarks and sleptons and c_H for soft Higgses. This choice of model parameters is denoted as a blue dot on the (α, M_0) plane of Fig.1, which was taken from the figure 12 (c) in ref.[12]. In the Fig.1, the magenta stripe corresponds to the parameter region giving a thermal relic density consistent with the recent WMAP observation [17], *i.e.* $0.085 < \Omega_{DM}h^2 < 0.119$. The benchmark point is also consistent with constraints on particle spectra and $b \to s\gamma$ branching ratio.

The SUSY particle mass spectrum at the electroweak(EW) scale was computed by solving the RG equations with the model parameter set (10). For the gluino and the first two generation squark masses, we find

$$m_{\tilde{g}} = 884.4\ \text{GeV},\ m_{\tilde{d}_L(\tilde{u}_L)} = 776.0\ (771.9)\ \text{GeV},\ m_{\tilde{d}_R(\tilde{u}_R)} = 733.5\ (741.8)\ \text{GeV}, \tag{11}$$

while the masses of the third generation squarks are

$$m_{\tilde{b}_{1(2)}} = 703.9\ (734.6)\ \text{GeV},\ m_{\tilde{t}_{1(2)}} = 545.3\ (782.0)\ \text{GeV} \tag{12}$$

On the other hand, the slepton and sneutrino masses are

$$m_{\tilde{e}_{R(L)}} = 382.0\ (431.5)\ \text{GeV},\ m_{\tilde{\tau}_{1(2)}} = 378.9\ (435.4)\ \text{GeV},\ m_{\tilde{\nu}_L} = 424.1\ \text{GeV}. \tag{13}$$

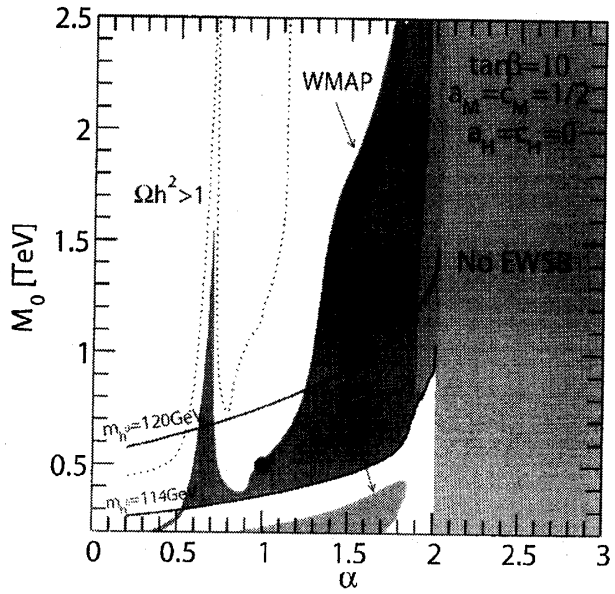

Figure 1: *Parameter space* (α, M_0) *with* $a_H = c_H = 0$, $a_M = c_M = 1/2$ *and* $\tan\beta = 10$. *The blue point corresponds to our benchmark point, which satisfy relic density bound of WMAP observation and is consistent with other experimental constraints on particle masses and* $b \to s\gamma$ *branching ratio.*

For the neutralino and chargino masses, we have

$$m_{\tilde{\chi}^0_{1,2,3,4}} = \{355.1,\ 416.1,\ 478.7,\ 535.6\}\ \text{GeV},\ m_{\tilde{\chi}^\pm_{1,2}} = \{408.2,\ 533.5\}\ \text{GeV}, \tag{14}$$

which correspond to the following bino,wino and Higgsino masses at electroweak scale,

$$M_1 = 367\ \text{GeV},\ M_2 = 461\ \text{GeV},\ \mu = 475\ \text{GeV}\ \ (\text{for}\ \tan\beta = 10). \tag{15}$$

Finally, Higgs masses are given by

$$m_h = 115\ \text{GeV}, m_H = 528.6\ \text{GeV}, m_A = 528.3\ \text{GeV}, m_{H^\pm} = 534.4\ \text{GeV}. \tag{16}$$

Fig. 2(a) shows the mass spectrum for the benchmark point. For comparison, we also show the spectrum of a mSUGRA point, which gives the same mass of neutralino LSP as the benchmark point, in Fig.2(b). One can notice that the spectrum of the benchmark point is quite degenerated, compared to the mSUGRA point.

With these mass parameters for the benchmark point, the neutralino LSP turns out to be bino-like, *but* with non-negligible wino and Higgsino components. Neutralino pair annihilation into a gauge boson pair (ZZ or W^+W^-) is then efficient so that thermal relic density of the neutralino LSP satisfies WMAP bound though the LSP is rather heavy ($m_{\tilde{\chi}^0_1} \sim 355$ GeV).

For the benchmark point, the ratio of gaugino masses at EW scale is given by $M_1 : M_2 : M_3 = 367 : 461 : 850 \simeq 1 : 1.26 : 2.32$, which is quite degenerated comparing to the typical ratio $M_1 : M_2 : M_3 \simeq 1 : 2 : 6$ for mSUGRA-like scenarios in which gaugino masses are unified at the GUT scale. For the benchmark point, the mass ratio of the gluino to the lightest neutralino is given by $m_{\tilde{g}}/m_{\tilde{\chi}^0_1} \simeq 2.5$, which is different from the typical mSUGRA predictions $m_{\tilde{g}}/m_{\tilde{\chi}^0_1} \geq 6$ and therefore implies that the gaugino masses are NOT unified at the GUT scale. In the next subsection, we will see the mass ratio $m_{\tilde{g}}/m_{\tilde{\chi}^0_1}$ can be measured experimentally so that we can get some information on SUSY breaking sector.

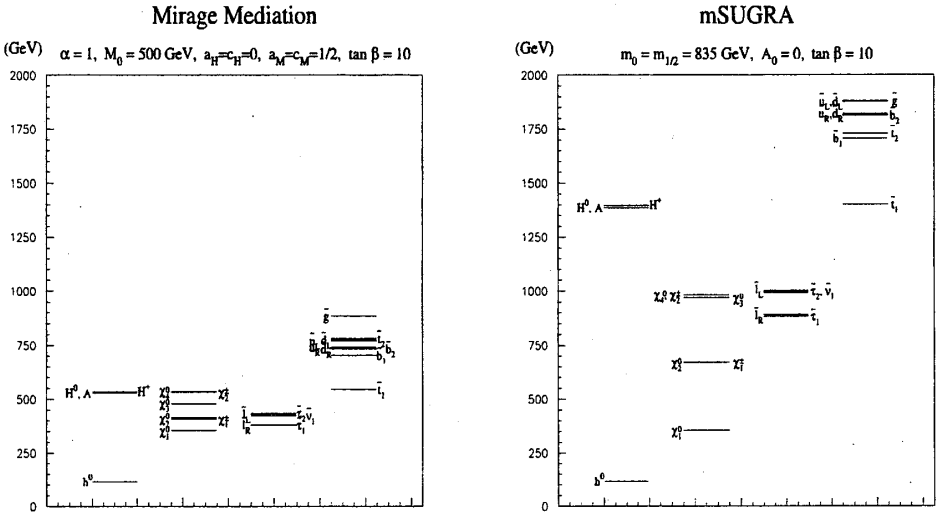

Figure 2: *The mass spectrum for (a) the benchmark point in mirage mediation and (b) a mSUGRA point. Both cases give the same mass for the lightest neutralino.*

2.2.2 Monte Carlo Events

A Monte Carlo event sample of the SUSY signals for proton-proton collision at an energy of 14 TeV has been generated by PYTHIA 6.4 [18]. The event sample corresponds to 30 fb^{-1} of integrated luminosity, which is expected with the 3 year running of the LHC at low luminosity. We have also generated SM background events *i.e.*, $t\bar{t}$ events equivalent to 30 fb^{-1} of integrated luminosity and also $W/Z+jet$, $WW/WZ/ZZ$ and QCD events, with less equivalent luminosity, in five logarithmic p_T bins for 50 GeV $< p_T <$ 4000 GeV. The generated events have been further processed with a modified version of the fast detector simulation program PGS (Pretty Good Simulation)[19], which approximate an ATLAS- or CMS-like detector with reasonable efficiencies and fake rates.

The total production cross section for SUSY events at the LHC is ∼6.1 pb for the benchmark point, corresponding to $\sim 1.8 \times 10^5$ events with 30 fb^{-1} luminosity. Squarks and gluinos are expected to be copiously produced at the LHC, if $m_{\tilde{q}}$, $m_{\tilde{g}} < 1$ TeV. With the masses of gluino and squarks in the Eq. (11), the production cross sections for the $\tilde{g}\tilde{g}$, $\tilde{g}\tilde{q}$, and $\tilde{q}\tilde{q}$ pairs are about 0.3 pb, 2.7 pb and 2.0 pb, respectively, such that the gluino-squark pair production and the squark pair production dominate.

The produced squarks and gluinos decay generally in multistep. In the recent past, the following cascade decay chain of squark has been exploited in detail [15, 16];

$$\tilde{q}_L \to \tilde{\chi}_2^0 q \to \tilde{l}_R^{\pm}\, l^{\mp} q \to \tilde{\chi}_1^0 l^+ l^- q, \tag{17}$$

especially in mSUGRA framework. It has been shown that it would be possible to reconstruct both upper edges for the l^+l^-, l^+l^-q, and $l^{\pm}q$ mass distribution and a lower edge for the l^+l^-q mass coming from backwards decays of the $\tilde{\chi}_2^0$ in the $\tilde{q}_L$ rest frame. Those edge values of the mass distributions are given by the following analytic formulae, in terms of the particle masses

involved in the decay chain;

$$M_{ll}^{max} = \left[\frac{(m^2_{\tilde{\chi}^0_2} - m^2_{\tilde{l}_R})(m^2_{\tilde{l}_R} - m^2_{\tilde{\chi}^0_1})}{m^2_{\tilde{l}_R}}\right]^{1/2}, \tag{18}$$

$$M_{llq}^{max} = \left[\frac{(m^2_{\tilde{q}_L} - m^2_{\tilde{\chi}^0_2})(m^2_{\tilde{\chi}^0_2} - m^2_{\tilde{\chi}^0_1})}{m^2_{\tilde{\chi}^0_2}}\right]^{1/2}, \tag{19}$$

$$M_{lq}^{max}(high) = \left[\frac{(m^2_{\tilde{q}_L} - m^2_{\tilde{\chi}^0_2})(m^2_{\tilde{\chi}^0_2} - m^2_{\tilde{l}_R})}{m^2_{\tilde{\chi}^0_2}}\right]^{1/2}, \tag{20}$$

$$\begin{aligned}(M_{llq}^{min})^2 &= \frac{1}{4m^2_{\tilde{\chi}^0_2}m^2_{\tilde{l}_R}}[- m^2_{\tilde{\chi}^0_1}m^4_{\tilde{\chi}^0_2} + 3m^2_{\tilde{\chi}^0_1}m^2_{\tilde{\chi}^0_2}m^2_{\tilde{l}_R} - m^4_{\tilde{\chi}^0_2}m^2_{\tilde{l}_R} - m^2_{\tilde{\chi}^0_2}m^4_{\tilde{l}_R} \\ &- m^2_{\tilde{\chi}^0_1}m^2_{\tilde{\chi}^0_2}m^2_{\tilde{q}_L} - m^2_{\tilde{\chi}^0_1}m^2_{\tilde{l}_R}m^2_{\tilde{q}_L} + 3m^2_{\tilde{\chi}^0_2}m^2_{\tilde{l}_R}m^2_{\tilde{q}_L} - m^4_{\tilde{l}_R}m^2_{\tilde{q}_L} \\ &+ (m^2_{\tilde{\chi}^0_2} - m^2_{\tilde{q}_L})\sqrt{(m^4_{\tilde{\chi}^0_1} + m^4_{\tilde{l}_R})(m^2_{\tilde{\chi}^0_2} + m^2_{\tilde{l}_R})^2 + 2m^2_{\tilde{\chi}^0_1}m^2_{\tilde{l}_R}(m^4_{\tilde{\chi}^0_2} - 6m^2_{\tilde{\chi}^0_2}m^2_{\tilde{l}_R} + m^4_{\tilde{l}_R})}\ ].\end{aligned} \tag{21}$$

We can also measure the upper edge of the distribution of the *smaller* of the two possible lq masses formed by combining two leptons with a quark jet [20];

$$\begin{aligned}M_{lq}^{max}(low) &= \left[\frac{(m^2_{\tilde{q}_L} - m^2_{\tilde{\chi}^0_2})(m^2_{\tilde{e}_R} - m^2_{\tilde{\chi}^0_1})}{2m^2_{\tilde{e}_R} - m^2_{\tilde{\chi}^0_1}}\right]^{1/2} \quad \text{for } 2m^2_{\tilde{e}_R} - (m^2_{\tilde{\chi}^0_1} + m^2_{\tilde{\chi}^0_2}) < 0. \\ &= \left[\frac{(m^2_{\tilde{q}_L} - m^2_{\tilde{\chi}^0_2})(m^2_{\tilde{\chi}^0_2} - m^2_{\tilde{e}_R})}{m^2_{\tilde{\chi}^0_2}}\right]^{1/2} \quad \text{for } 2m^2_{\tilde{e}_R} - (m^2_{\tilde{\chi}^0_1} + m^2_{\tilde{\chi}^0_2}) > 0.\end{aligned} \tag{22}$$

From the kinematic edge measurements, the SUSY particle masses might be then determined without relying on a model. For the benchmark point, we can notice that $m_{\tilde{\chi}^0_2} > m_{\tilde{e}_R}$. Therefore, the cascade decay chain (17) is indeed open so that the well-established method of the kinematic edge measurements can be applied to our case.

To reduce the SM background to a negligible level, we apply the following event selection cuts;

(1) At least three jets with $P_{T1} > 200$ GeV and $P_{T2,3} > 50$ GeV.
(2) Missing transverse energy, $E_T^{miss} > 200$ GeV.
(3) $E_T^{miss}/M_{eff} > 0.2$, where $M_{eff} \equiv P_{T1} + P_{T2} + P_{T3} + P_{T4} + E_T^{miss} + \sum_{leptons} P_{Tl}$
(4) At least two isolated leptons of opposite charge, with $P_T > 10$ GeV and $|\eta| < 2.5$.
(5) Transverse sphericity $S_T > 0.1$.
(6) No b-jets.

Following the analysis in Ref.[15], we have then calculated various invariant mass distributions for the benchmark point. The dilepton invariant mass distribution is shown in the Fig. 3. Here, the $e^+e^- + \mu^+\mu^- - e^\pm\mu^\mp$ combination was used in order to cancel contributions for two independent decays and reduce combinatorial background. The SM backgrounds which denoted as blue histogram on the plot, are negligible with the above event selection cuts, as expected from previous studies [13, 15]. We find a clear end point in the dilepton mass distribution. A Gaussian-smeared triangular fit to the distribution gives $M_{ll}^{max} = 60.61 \pm 0.13$

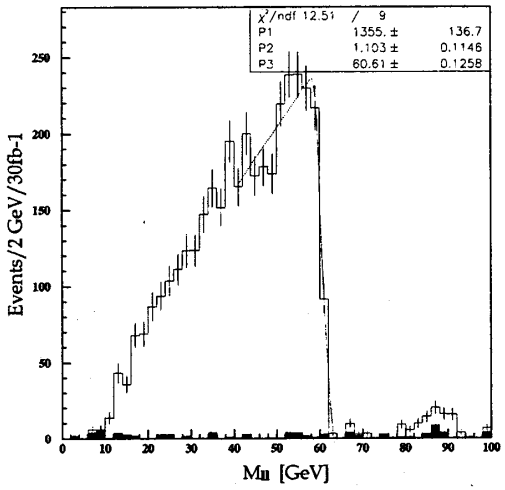

Figure 3: *Dilepton ($e^+e^- + \mu^+\mu^- - e^\pm\mu^\mp$) invariant mass distributions for the benchmark point. Blue histogram corresponds to SM background.*

GeV, which is $\sim 0.3\%$ lower than the calculated value of $M_{ll}^{max} = 60.8$ GeV for the decays $\tilde{\chi}_2^0 \to \tilde{l}_R l^\pm \to \tilde{\chi}_1^0 l^+ l^-$.

The dilepton plus jet invariant mass M_{llq} has been also calculated by combining the dilepton with one of the two hardest P_T jets. The two hardest jets are expected to come from squark decays $\tilde{q} \to \tilde{\chi} q$ as dominant production processes result in a pair of squark . The distribution for the smaller of the two possible llq masses is shown in Fig. 4(a). The upper edge value of the l^+l^-q masses is given by $M_{llq}^{max} = 341.5 \pm 3.6$ GeV, which is obtained from a Gaussian smeared fit plus a linear background. The fitted value is consistent with the calculated value of $M_{llq}^{max} = 341.4$ GeV for the decays $\tilde{q}_L \to \tilde{\chi}_2^0 q \to \tilde{l}_R^\pm l^\mp q \to \tilde{\chi}_1^0 l^+ l^- q$ (with $m_{\tilde{q}_L} = 776$ GeV).

Now, we further require that one M_{llq} should be less than 350 GeV and the other greater. Two $l^\pm q$ masses are then calculated using the combination of l^+l^-q with the smaller M_{llq} ($<$ 350 GeV). Fig. 4(b) shows the mass distribution of the *larger* of the two $l^\pm q$ system. A fit to the mass distribution near the end point is also shown, which yield an upper edge value $M_{lq}^{max}(high) = 258.6 \pm 4.8$ GeV, which is consistent with the calculated value of $M_{lq}^{max}(high) =$ 259.7 GeV.

The mass distribution of the *smaller* of the two M_{lq} is shown in Fig. 4(c). The upper edge value of the distribution from a linear fit is given by $M_{lq}^{max}(low) = 227.6 \pm 3.3$ GeV, which is consistent with the calculated value of $M_{lq}^{max}(low) = 226.5$ GeV.

The lower edge for l^+l^-q mass can be reconstructed from the larger of the two possible l^+l^-q masses, with additional requirement $M_{ll}^{max}/\sqrt{2} < M_{ll} < M_{ll}^{max}$. The resulting distribution is shown in Fig. 4(d). A fit to the distribution gives $M_{llq}^{min} = 145.3 \pm 2.8$ GeV, which is consistent with the generated value $M_{llq}^{min} = 145.4$ GeV.

From the above five edge measurements for the $\tilde{q}_L$ cascade decays (17), we can determine the masses of $\tilde{q}_L$, $\tilde{l}_R$, $\tilde{\chi}_2^0$ and $\tilde{\chi}_1^0$ using the eqs. (18-22).

With given masses of $\tilde{\chi}_1^0$ and $\tilde{\chi}_2^0$, we can get information for gluino and squark masses from

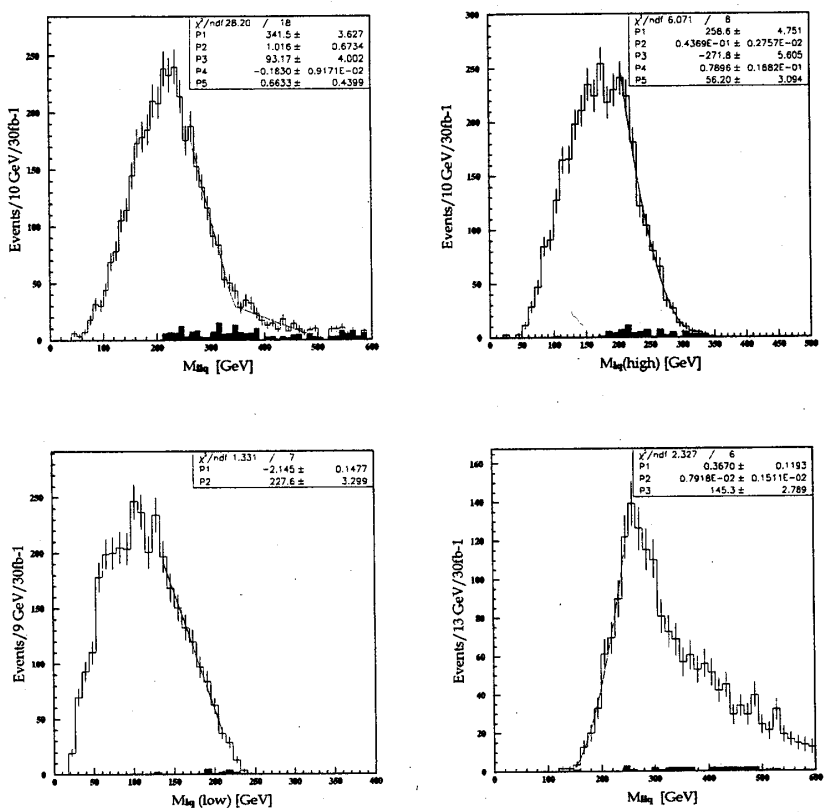

Figure 4: *Distributions for (a) the smaller of the two M_{llq}, (b) the larger of two M_{lq}, (c) the smaller of the two M_{lq}, and (d) the larger of the two M_{llq} with $M_{ll} > M_{ll}^{max}/\sqrt{2}$.*

the following gluino decay into right-handed squark plus quark;

$$\tilde{g} \to \tilde{q}_R q \to \tilde{\chi}_1^0 q q. \tag{23}$$

The maximal value of the two jet invariant mass for the gluino decays (23) is given by

$$M_{qq}^{max} = \left[\frac{(m_{\tilde{g}}^2 - m_{\tilde{q}_R}^2)(m_{\tilde{q}_R}^2 - m_{\tilde{\chi}_1^0}^2)}{m_{\tilde{q}_R}^2} \right]^{1/2}. \tag{24}$$

At the LHC, gluino would be produced mainly from $\tilde{g}\tilde{q}$ or $\tilde{g}\tilde{g}$ pair production. In order to obtain event sample for the gluino decay (23), the following event selection cuts are imposed;

(1) At least 3 jets with $P_{T1} > 200$ GeV, $P_{T2} > 150$ GeV and $P_{T3} > 100$ GeV.
(2) $E_T^{miss} > 350$ GeV and $E_T^{miss}/M_{eff} > 0.25$.
(3) Transverse sphericity $S_T > 0.15$.
(4) No b-jets and No leptons.

In the selection cuts, we required rather hard $P_{T3} > 100$ GeV in order to reduce $\tilde{q}\tilde{q}$ production events. After the selection cuts, we calculate dijet invariant mass M_{qq} using the three hardest jets. The smallest M_{qq} among the three possible combinations is then shown in Fig. 5 (a). The M_{qq} distribution is fitted near end point by a Gaussian smeared linear function with

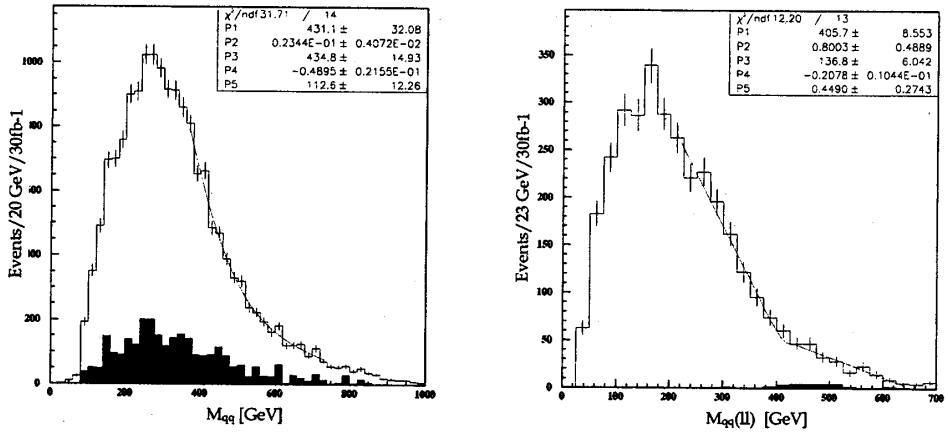

Figure 5: *Dijet invariant mass distribution (a) without dilepton and (b) with dilepton.*

a linear background. The resulting edge value is given by $M_{qq}^{max} = 431.1 \pm 32.1$ GeV, which is consistent with the calculated one $M_{qq}^{max} = 432.4$ GeV (with $m_{\tilde{q}_R} = 733.5$ GeV).

Additional information on $m_{\tilde{g}}$ and $m_{\tilde{q}_R}$ might be provided by the following cascade decay of gluino,

$$\tilde{g} \to \tilde{q}_R q \to \tilde{\chi}_2^0 qq \ (\to \tilde{\chi}_1^0 llqq), \tag{25}$$

for which the upper edge value of the two jet invariant mass distribution is given by

$$M_{qq}^{max}(ll) = \left[\frac{(m_{\tilde{g}}^2 - m_{\tilde{q}_R}^2)(m_{\tilde{q}_R}^2 - m_{\tilde{\chi}_2^0}^2)}{m_{\tilde{q}_R}^2} \right]^{1/2}. \tag{26}$$

In the gluino cascade decay (25), we consider the right-handed squark decay into $\tilde{\chi}_2^0$ rather than $\tilde{\chi}_1^0$, where the $\tilde{\chi}_2^0$ further undergoes the dileptonic decay. In the benchmark point, branching ratio $BR(\tilde{q}_R \to \tilde{\chi}_2^0 q) = 11\%$ is comparable to $BR(\tilde{q}_L \to \tilde{\chi}_2^0 q) = 18.5\%$. This is because the gaugino masses are quite degenerated (*i.e.* $M_2/M_1 \sim 1.26$) at EW scale so that $\tilde{\chi}_2^0$ has sizable bino-component in the benchmark point, which is in contrast to the typical mSUGRA case where $\tilde{\chi}_2^0$ is almost wino-like and therefore $BR(\tilde{q}_R \to \tilde{\chi}_2^0 q)$ is negligible. Furthermore, the gluino branching ratio of $BR(\tilde{g} \to \tilde{q}_R q) \simeq 19\%$ is larger than $BR(\tilde{g} \to \tilde{q}_L q) \simeq 11.2\%$ for q=u,d so that the decay chain of $\tilde{g} \to \tilde{q}_R q \to \tilde{\chi}_2^0 qq$ is comparable to that of $\tilde{g} \to \tilde{q}_L q \to \tilde{\chi}_2^0 qq$. Considering the squark masses that $m_{\tilde{q}_R} < m_{\tilde{q}_L}$, the upper edge value of two jet invariant mass for $\tilde{\chi}_2^0 qq$ events is essentially determined by the Eq. (26), which involves $m_{\tilde{q}_R}$ rather than $m_{\tilde{q}_L}$.

In order to select events which include decay chain (25), we require

(1) At least 3 jets with $P_{T1} > 200$ GeV and $P_{T2,3} > 50$ GeV
(2) $E_T^{miss} > 200$ GeV and $M_{eff}/E_T^{miss} > 0.2$
(3) At least two isolated leptons with opposite charge
(4) $M_{ll} < 61$ GeV and the smallest $M_{llq} < 350$ GeV
(5) Transverse sphericity $S_T > 0.1$
(6) No b-jets

After the selection cut, dijet invariant mass was calculated using the jet, which gives the smallest M_{llq}, with third and fourth (if any) energetic jets. The smaller of the two possible dijet mass is then shown in Fig. 5 (b). A fit to the distribution gives $M_{qq}^{max}(ll) = 405.7 \pm 8.6$ GeV, which is consistent with the calculated value of $M_{qq}^{max}(ll) = 406.9$ GeV (with $m_{\tilde{q}_R} = 733.5$ GeV).

The upper edge measurements of two dijet invariant masses provide lower limits on the gluino and squark masses and a strong correlation between $m_{\tilde{g}}$ and $m_{\tilde{q}_R}$, but without constraint on the upper limit on the masses. In order to further constrain the right-handed squark mass,

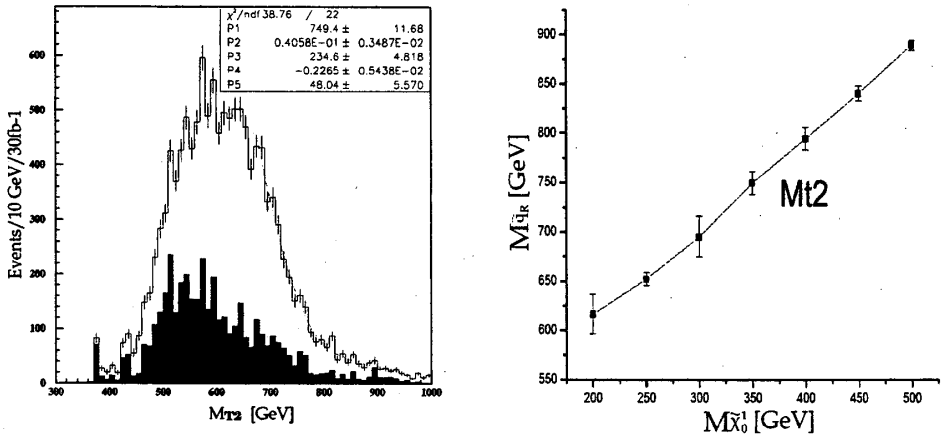

Figure 6: *(a) The M_{T2} distribution with the input value of $m_\chi = 350$ GeV as an example. (b) A relation between $m_{\tilde{q}_R}$ and $m_{\tilde{\chi}_1^0}$ from the M_{T2} analysis.*

we consider squark pair production and their subsequent decay into two quarks plus two LSPs;

$$\tilde{q}_{1R}\tilde{q}_{2R} \to q_1\tilde{\chi}_1^0 q_2\tilde{\chi}_1^0, \tag{27}$$

and construct another variable M_{T2} [21], which is defined by

$$M_{T2}^2 \equiv \min_{\mathbf{p}_{T1}^\chi + \mathbf{p}_{T2}^\chi = \mathbf{p}_T^{miss}} \left[\max\{m_T^2(\mathbf{p}_T^{q_1}, \mathbf{p}_{T1}^\chi), m_T^2(\mathbf{p}_T^{q_2}, \mathbf{p}_{T2}^\chi)\}\right], \tag{28}$$

where

$$m_T^2(\mathbf{p}_T^q, \mathbf{k}_T^\chi) \equiv m_q^2 + m_\chi^2 + 2(E_T^q E_T^\chi - \mathbf{p}_T^q \cdot \mathbf{k}_T^\chi), \tag{29}$$

$$E_T^q = \sqrt{|\mathbf{p}_T^q|^2 + m_q^2}, \quad E_T^\chi = \sqrt{|\mathbf{k}_T^\chi|^2 + m_\chi^2}. \tag{30}$$

Here, $\mathbf{p}_T^{q_1}$ and $\mathbf{p}_T^{q_2}$ denote the transverse momentum of quark-jets from the squark decays and $\mathbf{p}_T^{miss}$ is the observed missing transverse momentum and m_χ is an estimate of the lightest neutralino mass. The M_{T2} distribution has an endpoint at the squark mass $m_{\tilde{q}_R}$ when the input m_χ is equal to the correct $m_{\tilde{\chi}_1^0}$ value. In general we obtain a relation between $m_{\tilde{q}_R}$ and $m_{\tilde{\chi}_1^0}$.

In order to have event sample for the squark pair production and their subsequent decay (27), the following event selection cuts are required;

(1) At least two jets with $P_{T1} > 300$ GeV, $P_{T2} > 50$ GeV

(2) $E_T^{miss} > 200$ GeV, $M_{eff}/E_T^{miss} > 0.3$

(3) Transverse sphericity $S_T > 0.15$

(4) No leptons, no b-jets.

Fig. 6(a) shows an example of M_{T2} distribution with an input value of $m_\chi = 350$ GeV. From a fit to the distribution, we obtain $m_{\tilde{q}_R} = 749 \pm 12$ GeV for the example. A general relation between $m_{\tilde{q}_R}$ and $m_{\tilde{\chi}_1^0}$ from the M_{T2} analysis is shown in Fig. 6(b).

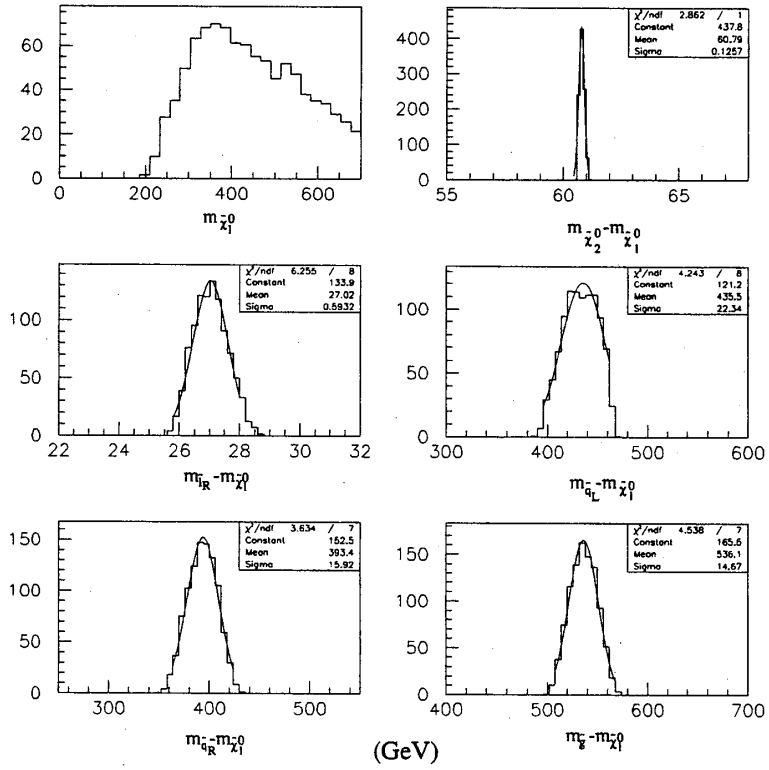

Figure 7: *Probability distribution of (a)* $m_{\tilde{\chi}_1^0}$, *(b)* $m_{\tilde{\chi}_2^0} - m_{\tilde{\chi}_1^0}$, *(c)* $m_{\tilde{l}_R} - m_{\tilde{\chi}_1^0}$, *(d)* $m_{\tilde{q}_L} - m_{\tilde{\chi}_1^0}$, *(e)* $m_{\tilde{q}_R} - m_{\tilde{\chi}_1^0}$ *and (f)* $m_{\tilde{g}} - m_{\tilde{\chi}_1^0}$.

Now we can determine six SUSY particle masses, $m_{\tilde{\chi}_1^0}$, $m_{\tilde{\chi}_2^0}$, $m_{\tilde{l}_R}$, $m_{\tilde{q}_L}$, $m_{\tilde{g}}$ and $m_{\tilde{q}_R}$, from the various kinematic distributions we considered so far. In order to scan possible values of SUSY particle masses, random numbers for $m_{\tilde{\chi}_2^0}$, $m_{\tilde{l}_R}$, $m_{\tilde{q}_L}$, $m_{\tilde{q}_R}$, and $m_{\tilde{g}}$ were generated within some ranges around their nominal values, while $m_{\tilde{\chi}_1^0}$ values were calculated with the measured M_{ll}^{max} value. The chi-square from the various kinematic observables with their errors was calculated to determine the probability for each set of masses. Fig. 7 shows the probability distribution of (a) $m_{\tilde{\chi}_1^0}$, (b) $m_{\tilde{\chi}_2^0} - m_{\tilde{\chi}_1^0}$, (c) $m_{\tilde{l}_R} - m_{\tilde{\chi}_1^0}$ (d) $m_{\tilde{q}_L} - m_{\tilde{\chi}_1^0}$, (e) $m_{\tilde{q}_R} - m_{\tilde{\chi}_1^0}$ and (f) $m_{\tilde{g}} - m_{\tilde{\chi}_1^0}$, respectively. While the $\tilde{\chi}_1^0$ mass is determined as

$$m_{\tilde{\chi}_1^0} = 356^{+220}_{-95} \text{ GeV}, \tag{31}$$

the differences between sparticle masses are rather well constrained,

$$\begin{aligned} m_{\tilde{\chi}_2^0} - m_{\tilde{\chi}_1^0} &= 60.8 \pm 0.1 \text{ GeV}, \; m_{\tilde{l}_R} - m_{\tilde{\chi}_1^0} = 27.0 \pm 0.6 \text{ GeV}, \; m_{\tilde{q}_L} - m_{\tilde{\chi}_1^0} = 436 \pm 22 \text{ GeV}, \\ m_{\tilde{q}_R} - m_{\tilde{\chi}_1^0} &= 393 \pm 16 \text{ GeV}, \; m_{\tilde{g}} - m_{\tilde{\chi}_1^0} = 536 \pm 15 \text{ GeV}, \end{aligned} \tag{32}$$

respectively. The central values for the estimated masses are consistent with the generated ones. And the range for the mass ratio between gluino and the lightest neutralino is given by

$$1.9 < \frac{m_{\tilde{g}}}{m_{\tilde{\chi}_1^0}} < 3.1 \quad (\textit{reduced } \chi^2 < 1), \tag{33}$$

which is quite distinctive from the typical predictions *i.e.*, $m_{\tilde{g}}/m_{\tilde{\chi}_1^0} \geq 6$ of the other SUSY scenarios in which gaugino masses are unified at GUT scale.

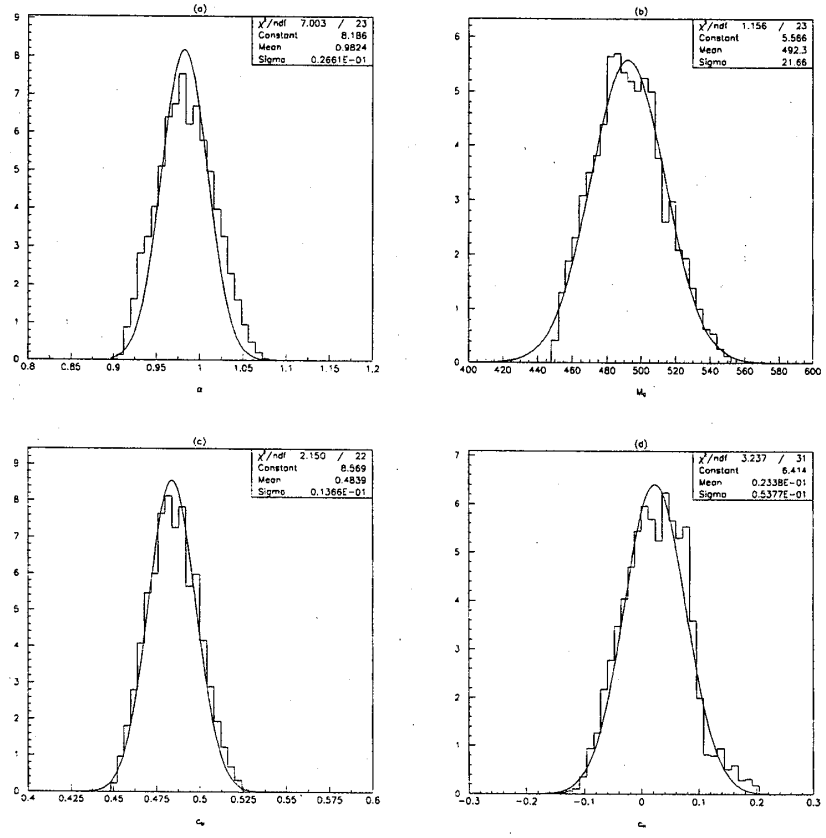

Figure 8: *Probability distribution of (a) α, (b) M_0, (c) c_M, and (d) c_H.*

So far we have considered 'model-independent' measurements of SUSY particle masses. We can also determine the model parameters of mirage mediation scenario from the kinematic endpoint measurements. As mentioned in section 2.1, generic mirage mediation is parameterized by M_0, α, a_i, c_i and $\tan\beta$. Here, we assume that visible sfermion fields have a universal parameter $c_M (= a_M)$ while the corresponding parameter for Higgs fields is given by $c_H (= a_H)$. The model is then described by five parameters M_0, α, c_M, c_H and $\tan\beta$. From the Eq. (8) and (9) we can see that the gaugino and the first generation sfermion masses at low energy scale are essentially

determined by M_0, α and c_M. Therefore, we can determine the model parameters M_0, α and c_M from the measured $m_{\tilde{g}}, m_{\tilde{q}}$ and $m_{\tilde{l}_R}$. With given values of M_0, α and c_M, the parameters c_H and tanβ might be obtained from the measured $m_{\tilde{\chi}_1^0}$ and $m_{\tilde{\chi}_2^0}$. We have scanned five model parameters in certain ranges and calculated the χ^2 from the calculated and measured kinematic edge values, in order to constraint the model parameters. Fig. 8 shows probability distributions for α,M_0,c_M and c_H, resulting in the following values of the parameters:

$$\alpha = 0.98 \pm 0.03,\ M_0 = 492 \pm 22\ \text{GeV},\ c_M = 0.48 \pm 0.01,\ c_H = 0.02 \pm 0.05. \tag{34}$$

The model parameters are determined quite accurately, except tanβ whose value is not so well constrained because neutralino masses depend on it rather mildly. The resulting central values of the parameters well agree with the input values of Eq (10).

3 Tau polarization in SUSY cascade decay

Much attention has been paid in the recent past to the SPS1a cascade [22]

$$\tilde{q} \ \rightarrow\ q\tilde{\chi}_2^0 \ \rightarrow\ q\ell\tilde{\ell} \ \rightarrow\ q\ell\ell\tilde{\chi}_1^0 \tag{35}$$

which gives rise to a well-populated ensemble of neutralinos and R-type sleptons with ratios of 30%, 10% and 100% in the first, second and third branching, respectively. Analyzing the visible $q\ell\ell$ final state in various combinations of leptons and quark jet, the cascade has served to study the precision with which the masses of supersymmetric particles can be measured at LHC, for a summary see Ref. [16]. In addition, invariant mass distributions have been shown sensitive to the spin of the particles involved [23, 24, 25, 26], shedding light on the very nature of the new particles observed in the cascade and on the underlying physics scenario.

So far, cascades have primarily been studied involving first and second generation leptons/sleptons. Here, we explore how the polarization of τ leptons can be exploited to study R/L chirality and mixing effects in both the $\tilde{\tau}$ and the neutralino sectors.[2] As expected, it turns out that measuring the correlation of the τ polarizations provides an excellent instrument to analyze these effects.

As polarization analyzer we will use single pion decays of the τ's. At high energies the mass of the τ leptons can be neglected and the fragmentation functions are linear in the fraction z of the energy transferred from the polarized τ's to the π's [28]:

$$(\tau_R)^\pm \ \rightarrow\ \overset{(-)}{\nu}_\tau\, \pi^\pm \ :\quad F_R \ =\ 2z \tag{36}$$

$$(\tau_L)^\pm \ \rightarrow\ \overset{(-)}{\nu}_\tau\, \pi^\pm \ :\quad F_L \ =\ 2(1-z) \tag{37}$$

In the relativistic limit, helicity and chirality are of equal and opposite sign for τ^- leptons and τ^+ anti-leptons, respectively. For notational convenience we characterize the τ states by chirality.

Pion distributions, summed over near and far particles, are predicted by folding the original single τ and double $\tau\tau$ distributions, $d\Gamma_\beta/dm^2_{q\tau}$ and $d\Gamma_{\beta\gamma}/dm^2_{\tau\tau}$, with the single and double fragmentation functions F_β and $F_{\beta\gamma}$, where the indices β, γ denote the chirality indices R/L of the τ leptons. Based on standard techniques, the following relations can easily be derived for $[q\pi]$ and $[\pi\pi]$ distributions:

$$\frac{d\Gamma}{dm^2_{q\pi}} \ =\ \int_{m^2_{q\pi}}^1 \frac{dm^2_{q\tau}}{m^2_{q\tau}} \frac{d\Gamma_\beta}{dm^2_{q\tau}}\, F_\beta\left(\frac{m^2_{q\pi}}{m^2_{q\tau}}\right) \tag{38}$$

[2]For a discussion of polarization effects in single τ decays see Ref.[27].

$$\frac{d\Gamma}{dm^2_{\pi\pi}} = \int_{m^2_{\pi\pi}}^1 \frac{dm^2_{\tau\tau}}{m^2_{\tau\tau}} \frac{d\Gamma_{\beta\gamma}}{dm^2_{\tau\tau}} F_{\beta\gamma}\left(\frac{m^2_{\pi\pi}}{m^2_{\tau\tau}}\right) \tag{39}$$

The single $\tau_\beta \to \pi$ fragmentation function, *cf.* Eqs. (36) and (37) with $z = m^2_{q\pi}/m^2_{q\tau}$, can be summarized as, with $\beta = \pm$ for R/L chirality,

$$F_\beta(z) = 1 + \beta\,(2z - 1) \tag{40}$$

while the double $\tau_\beta\tau_\gamma \to \pi\pi$ fragmentation functions, with $z = m^2_{\pi\pi}/m^2_{\tau\tau}$, are given by

$$F_{RR}(z) = 4\,z\,\log\frac{1}{z} \tag{41}$$

$$F_{RL}(z) = F_{LR}(z) = 4\left[1 - z - z\,\log\frac{1}{z}\right] \tag{42}$$

$$F_{LL}(z) = 4\left[(1+z)\,\log\frac{1}{z} + 2z - 2\right] \tag{43}$$

All distributions, normalized to unity, are finite except F_{LL} which is logarithmically divergent for $z \to 0$.

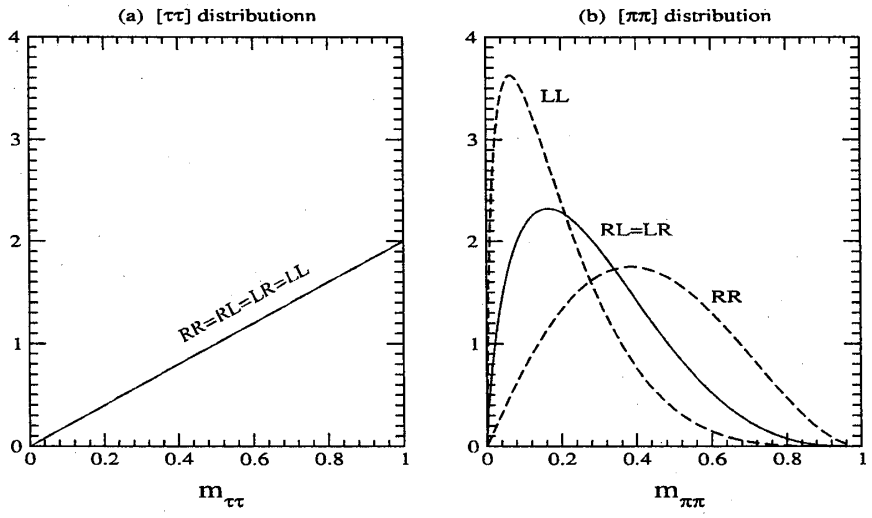

Figure 9: *The "normalized" invariant mass distributions of (a) $\tau\tau$ and (b) $\pi\pi$ pairings in the $\tilde{\chi}^0_2$ decays of the cascade (35). The indices denote the chiralities of the near and far tau leptons.*

The great potential of polarization measurements for determining spin and mixing phenomena is demonstrated in Figs. 9(a/b), displaying the invariant mass distribution of (a) $\tau\tau$ and (b) $\pi\pi$ pairings in the $\tilde{\chi}^0_2$ decays of the cascade (35). While the lepton-lepton invariant mass does not depend on the chirality indices of the near and far tau leptons τ_n and τ_f, the shape of the pion distribution depends strongly on the indices, as expected. This is also reflected in the expectation values of the invariant masses:

$$\langle m^2_{\pi\pi}\rangle = \begin{cases} 4/18 \\ 2/18 \\ 1/18 \end{cases} \quad \text{and} \quad \langle m_{\pi\pi}\rangle = \begin{cases} 288/675 & \text{for } RR \\ 192/675 & \text{for } RL/LR \\ 128/675 & \text{for } LL \end{cases} \tag{44}$$

which are distinctly different for the pion final states. Due to the scalar stau intermediate state, the $\tau\tau$ and $\pi\pi$ distributions do not depend on the polarization state of the parent $\tilde{\chi}_2^0$ state, contrary to the $q\tau$ and $q\pi$ distributions in the chain.

Cutting out small transverse pion momenta in actual experiments will modify the distributions of the $\pi\pi$ invariant mass, and the distributions are shifted to larger $m_{\pi\pi}$ values. For R chiralities of the τ's, with hard $\tau \to \pi$ fragmentation, the shift is smaller than for L chiralities with soft fragmentation.

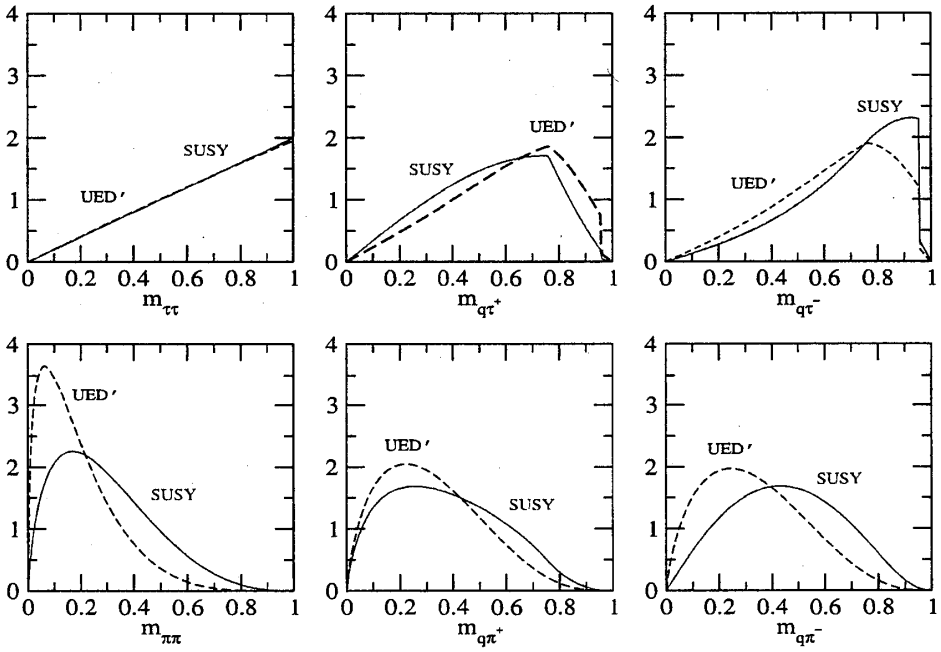

Figure 10: *The "normalized" distributions in supersymmetry and UED′ for the particle spectrum corresponding to the SUSY scenario SPS1a; the distributions* $[\tau\tau]$, $[q\tau^+]$ *and* $[q\tau^-]$ *in the upper frames and the distributions* $[\pi\pi]$, $[q\pi^+]$ *and* $[q\pi^-]$ *in the lower frames.*

The sensitivity of various distributions $[\tau\tau]$, $[q\tau^+]$, $[q\tau^-]$ and $[\pi\pi]$, $[q\pi^+]$, $[q\pi^-]$ in the cascade (35) starting with a left-handed squark $\tilde{q}_L$ is studied in the tableau of Fig. 10. The distributions are compared for the SUSY chain in SPS1a, in which the probability for $\tilde{\tau}_R$ in $\tilde{\tau}_1$ is close to 90%, with a spin chain (UED′) characteristic for universal extra-dimension models [31, 32]:

$$q_1 \;\to\; qZ_1 \;\to\; q\ell\ell_1 \;\to\; q\ell\ell\gamma_1 \tag{45}$$

To focus on the spin aspects,[3] the same mass spectrum is chosen in the UED′ as in the SUSY chain: $m_{\tilde{q}_L} = m_{q_1} = 570.6$ GeV, $m_{\tilde{\chi}_2^0} = m_{Z_1} = 176.4$ GeV, $m_{\tilde{\tau}_1} = m_{\tau_1} = 134.1$ GeV and $m_{\tilde{\chi}_1^0} = m_{\gamma_1} = 98.6$ GeV. The $[\tau\tau]$ distribution is linear $\sim m_{\tau\tau}$ in supersymmetry. It deviates slightly from the linear dependence in the $\tau\tau$ invariant mass in UED′ where in the limit of degenerate KK masses the distribution reads $\sim m_{\tau\tau}[1 - \frac{1}{5}m_{\tau\tau}^2]$. The kinks in the invariant mass distributions $[q\tau]$ and $[q\pi]$ signal the transition from near to far τ's and π's as the main

[3]For this purpose we deliberately ignore the naturally expected mass pattern in models of universal extra dimensions.

components of the events. Again, the best discriminant is the $[\pi\pi]$ distribution. This reflects the R-dominated character of $\tilde{\tau}$ as opposed to the L current coupled to the Kaluza-Klein state $Z_1 \simeq W^3$ [32].

Experimental analyses of τ particles are a difficult task at LHC. Isolation criteria of hadron and lepton tracks must be met which reduce the efficiencies strongly for small transverse momenta. Stringent transverse momentum cuts increase the efficiencies but reduce the primary event number and erase the difference between R and L distributions. On the other hand, fairly small transverse momentum cuts reduce the efficiencies but do not reduce the primary event number and the R/L sensitivity of the distributions. Optimization procedures in this context are far beyond the scope of this theoretical note. Experimental details may be studied in the recent reports[33, 2] in which the analysis of di-τ final states is presented for supersymmetry cascades of type (1) at LHC.

In Fig. 11(a) it is shown how a cut of 15 GeV on the pion transverse momenta modifies the SUSY and UED′ distributions of the $\pi\pi$ invariant mass. Given the specific SPS1a mass differences, the SUSY LR-dominated distribution is mildly affected while the UED′ LL-dominated distribution is shifted more strongly. The different size of the shifts can be traced back to the different shapes of the R and L fragmentation functions. Since L fragmentation is soft, more events with low transverse momentum are removed by the cut and the shift is correspondingly larger than for hard R fragmentation. Apparently, the transverse momentum cut does not erase the distinctive difference between the LR and LL distributions.

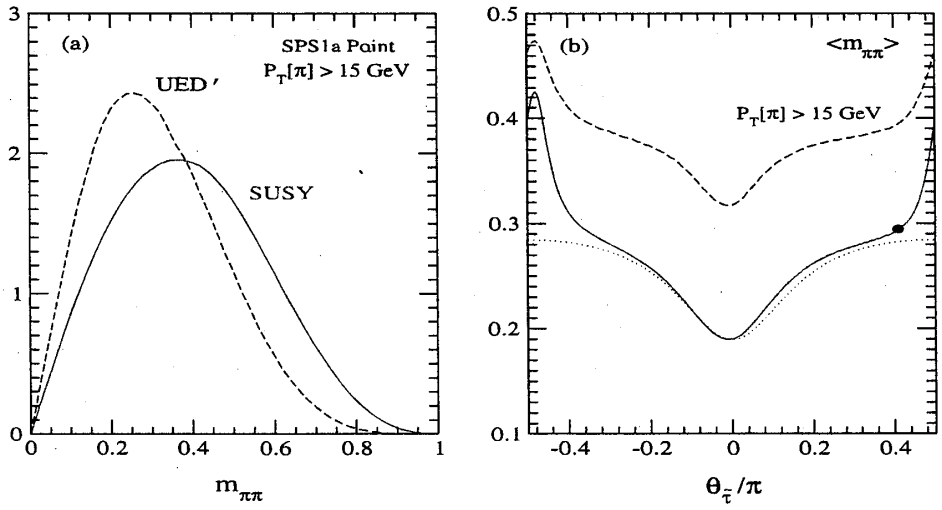

Figure 11: *(a) The SUSY and UED′ distributions of the $\pi\pi$ invariant mass with a cut of 15 GeV on the pion transverse momenta; and (b) the dependence of the expectation value $\langle m_{\pi\pi}\rangle$ on the stau mixing angle $\theta_{\tilde{\tau}}$ [in units of π] for the SPS1a values of $\tan\beta, M_{1,2}, \mu$ and the lighter stau mass $m_{\tilde{\tau}_1}$ [without (red) and with (blue) π transverse momentum cut]. The (red) dot on the solid line denotes the value of $\langle m_{\pi\pi}\rangle$ at the SPS1a point. The (red) dotted line represents the average values of $\langle m_{\pi\pi}\rangle$ if $\tilde{\chi}^0_{1,2}$ are unmixed pure bino-like and wino-like states, respectively.*

Finally we study the dependence of the $[\pi\pi]$ distribution on the stau mixing angle $\theta_{\tilde{\tau}}$, setting

all other parameters to their SPS1a values:

$$\tilde{\tau}_1 = \cos\theta_{\tilde{\tau}}\,\tilde{\tau}_L + \sin\theta_{\tilde{\tau}}\,\tilde{\tau}_R \quad (46)$$

$$\tilde{\tau}_2 = -\sin\theta_{\tilde{\tau}}\,\tilde{\tau}_L + \cos\theta_{\tilde{\tau}}\,\tilde{\tau}_R \quad (47)$$

The predictions for the $[\pi\pi]$ invariant-mass expectation value are shown in Fig. 11(b). The effect of a 15 GeV cut on the transverse momenta of the pions is included for comparison. The stau mixing angle of the SPS1a point, $\theta_{\tilde{\tau}} \approx 0.4\pi$, is indicated by the red dot in the figure, representing a state $\tilde{\tau}_1$ with 90% $\tilde{\tau}_R$ and 10% $\tilde{\tau}_L$ components. The large sensitivity of the $[\pi\pi]$ invariant mass to the mixing angle can be traced back to the fact that the neutralino $\tilde{\chi}^0_2$ is nearly wino-like ($N_{22} = -0.94$). For $\theta_{\tilde{\tau}} = \pm\pi/2$ the R state $\tilde{\tau}_1 = \tilde{\tau}_R$, couples to $\tilde{\chi}^0_2$ only through its small higgsino and U(1) gaugino components (*i.e.* $h_\tau N_{23} = 0.04$ and $N_{21} = -0.11$). However, once the mixing angle deviates slightly from $\pm\pi/2$ the "near" tau lepton τ_n coupling quickly becomes L-dominated. The cut on the pion transverse momenta modifies the $m_{\pi\pi}$ distribution, moderately for R chirality and strongly for L chirality. Nevertheless, for each chirality combination the shift is predicted completely in terms of the squark, $\tilde{\chi}^0_{1,2}$ and $\tilde{\tau}_1$ masses, and the shapes of the R/L fragmentation functions, so that it is under proper control. In particular, the relatively large increase of the average $\langle m_{\pi\pi}\rangle$ near $\theta_{\tilde{\tau}} = 0$ compared with $\pm\pi/2$ follows from the large effect of the transverse momentum cut due to the soft L fragmentation, *cf.* Fig. 11(b).

The analysis of τ polarization in cascade decays provides valuable information on chirality-type and mixing of supersymmetric particles. The most exciting effects are predicted for the invariant mass distributions in the $\pi\pi$ sector generated by the two polarized τ decays. This is strikingly different from the lepton-lepton invariant mass distributions in the first two generations which do not depend on the R and L couplings. It is particularly important to notice that these polarization effects are independent of the couplings in the squark/quark sector and also of the polarization state of the parent $\tilde{\chi}^0_2$ generating the final $\tau\tau\tilde{\chi}^0_1$ state.

4 Gluino m_{T2}

We introduce a new observable, 'gluino stransverse mass', which is an application of m_{T2} variable [21] to the process where gluinos are pair produced in proton-proton collision and each gluino subsequently decays into two quarks and one LSP,

$$pp \to \tilde{g}\tilde{g} \to qq\tilde{\chi}^0_1\, qq\tilde{\chi}^0_1. \quad (48)$$

We show that the gluino stransverse mass can be utilized to measure the gluino and the lightest neutralino masses separately, and also the (1st and 2nd generation) squark masses if lighter than the gluino mass, thereby providing a good first look at the pattern of sparticle masses experimentally.

If light enough, gluinos would be pair produced copiously in proton-proton collision ($pp \to \tilde{g}\tilde{g}$), and each gluino decays into two quarks and one LSP ($\tilde{g} \to qq\tilde{\chi}^0_1$) through three-body decay induced by an exchange of off-shell squark or two body cascade decay with intermedate on-shell squark. For each gluino decay $\tilde{g} \to qq\tilde{\chi}^0_1$, a transverse mass is constructed, which is defined as

$$m_T^2(m_{qqT}, m_\chi, \mathbf{p}_T^{qq}, \mathbf{p}_T^\chi) = m_{qqT}^2 + m_\chi^2 + 2(E_T^{qq}E_T^\chi - \mathbf{p}_T^{qq}\cdot\mathbf{p}_T^\chi), \quad (49)$$

where m_{qqT} and $\mathbf{p}_T^{qq}$ are the transverse invariant mass and transverse momentum of the qq system respectively, while m_χ and $\mathbf{p}_T^\chi$ are the *assumed* mass and transverse momentum of the

LSP, respectively. The transverse energies of the qq system and of the LSP are defined by

$$E_T^{qq} \equiv \sqrt{|\mathbf{p}_T^{qq}|^2 + m_{qqT}^2} \quad \text{and} \quad E_T^{\chi} \equiv \sqrt{|\mathbf{p}_T^{\chi}|^2 + m_{\chi}^2}, \tag{50}$$

respectively. With two sets of such a gluino decay in an event, the gluino stransverse mass $m_{T2}(\tilde{g})$ is defined by

$$m_{T2}^2(\tilde{g}) \equiv \min_{\mathbf{p}_T^{\chi(1)}+\mathbf{p}_T^{\chi(2)}=\mathbf{p}_T^{miss}} \left[\max\{m_T^{2(1)}, m_T^{2(2)}\}\right], \tag{51}$$

where the minimization is performed over all possible splittings of the observed missing transverse energy $\mathbf{p}_T^{miss}$ into two assumed transverse momenta, $\mathbf{p}_T^{\chi(1)}$ and $\mathbf{p}_T^{\chi(2)}$.

By the definition (51) of the gluino stransverse mass, one obtains a relation:

$$m_{T2}(\tilde{g}) \leq m_{\tilde{g}} \quad \text{for} \quad m_{\chi} = m_{\tilde{\chi}_1^0}, \tag{52}$$

i.e., $m_{T2}(\tilde{g})$ is less than or equal to true gluino mass $m_{\tilde{g}}$, if the *trial* LSP mass m_{χ} is equal to the *true* LSP mass $m_{\tilde{\chi}_1^0}$. Therefore one can determine $m_{\tilde{g}}$ from the endpoint measurement of $m_{T2}(\tilde{g})$ distribution:

$$m_{T2}^{\max}(m_{\chi}) \equiv \max_{\text{all events}} \left[m_{T2}(\tilde{g})\right], \tag{53}$$

if we already know the true LSP mass. However $m_{\tilde{\chi}_1^0}$ value might be unknown in advance and then, for a trial m_{χ} value which is different from $m_{\tilde{\chi}_1^0}$, $m_{T2}^{\max}(m_{\chi})$ will differ from $m_{\tilde{g}}$ and be given by a function of the mass m_{χ}.

As we will see, $m_{T2}^{\max}(m_{\chi})$ has different functional form depending upon whether the 1st and 2nd generation squarks are heavier or lighter than the gluino. Thus, in order to investigate the m_{χ}-dependence of $m_{T2}^{\max}$, let us consider two cases separately.

If squark masses are larger than gluino mass, the gluino will undergo three body decay into two quarks and an invisible LSP through the exchange of off-shell squark:

$$\tilde{g} \to qq\tilde{\chi}_1^0. \tag{54}$$

In order to get an idea how $m_{T2}^{\max}(m_{\chi})$ are determined for a generic value of the trial LSP mass m_{χ}, we consider two extreme momentum configurations and then construct the corresponding gluino stransverse mass for each of them.

The first momentum configuration considered is that two gluinos are produced at rest and then each gluino subsequently decays into two quarks which go to the same direction each other, and one LSP whose direction is opposite to the two quark system. Furthermore, two sets of gluino decay products are parallel to each other and all of them are on transverse plane with respect to proton beam direction. In the momentum configuration, we have

$$m_{qqT}^{(1)} = m_{qqT}^{(2)} = 0 \tag{55}$$

for *massless* quarks and the transverse energies and transverse momenta of the qq systems are given by

$$\begin{aligned} E_T^{qq}(max) &\equiv E_T^{qq(1)} = E_T^{qq(2)} \\ &= |\mathbf{p}_T^{qq(1)}| = |\mathbf{p}_T^{qq(2)}| = \frac{m_{\tilde{g}}^2 - m_{\tilde{\chi}_1^0}^2}{2m_{\tilde{g}}}, \end{aligned} \tag{56}$$

in terms of the true gluino mass $m_{\tilde{g}}$ and the true LSP mass $m_{\tilde{\chi}_1^0}$. And the total observed missing transverse momentum is given by $|\mathbf{p}_T^{miss}| = 2E_T^{qq}(max)$. The $m_{T2}(\tilde{g})$ can be obtained as the

minimum of $m_T^{(1)}$ subject to two constraints $m_T^{(1)} = m_T^{(2)}$ and $\mathbf{p}_T^{miss} = \mathbf{p}_T^{\chi(1)} + \mathbf{p}_T^{\chi(2)}$ [21]. From the two constraints, we obtain $\mathbf{p}_T^{\chi(1)} = \mathbf{p}_T^{\chi(2)} = \mathbf{p}_T^{miss}/2$ for the solution of the m_{T2} variable. Therefore the gluino stransverse mass is given by

$$m_{T2}(\tilde{g}) = E_T^{qq}(max) + \sqrt{(E_T^{qq}(max))^2 + m_\chi^2}. \tag{57}$$

for a generic m_χ. One can show that the above $m_{T2}(\tilde{g})$ corresponds to $m_{T2}^{\max}$ for $m_\chi \leq m_{\tilde{\chi}_1^0}$:

$$m_{T2}^{\max}(m_\chi) = \frac{m_{\tilde{g}}^2 - m_{\tilde{\chi}_1^0}^2}{2m_{\tilde{g}}} + \sqrt{\left(\frac{m_{\tilde{g}}^2 - m_{\tilde{\chi}_1^0}^2}{2m_{\tilde{g}}}\right)^2 + m_\chi^2} \quad \text{for} \quad m_\chi \leq m_{\tilde{\chi}_1^0}. \tag{58}$$

Note that $m_{T2}^{\max}(m_\chi = m_{\tilde{\chi}_1^0}) = m_{\tilde{g}}$ as anticipated.

Other extreme momentum configuration which would determine $m_{T2}^{\max}(m_\chi)$ for $m_\chi \geq m_{\tilde{\chi}_1^0}$ is that gluinos are pair produced at rest and for each gluino decay, two quarks are back to back each other while LSP is at rest. In addition, all particles are on the transverse plane. In this case, one easily finds

$$m_{qqT}(max) \equiv m_{qqT}^{(1)} = m_{qqT}^{(2)} = m_{\tilde{g}} - m_{\tilde{\chi}_1^0}, \tag{59}$$

and also $E_T^{qq(1)} = E_T^{qq(2)} = m_{qqT}(max)$ because $\mathbf{p}_T^{qq(1)} = \mathbf{p}_T^{qq(2)} = 0$. Then $m_T^{(1)}$ is always equal to $m_T^{(2)}$ for all possible splitting of the missing transverse momentum; $\mathbf{p}_T^{miss} = 0 = \mathbf{p}_T^{\chi(1)} + \mathbf{p}_T^{\chi(2)}$. The minimum of $m_T^{(1)} (= m_T^{(2)})$ occurs when $\mathbf{p}_T^{\chi(1)} = \mathbf{p}_T^{\chi(2)} = 0$, therefore the gluino stransverse mass is given by

$$m_{T2}(\tilde{g}) = m_{qqT}(max) + m_\chi \tag{60}$$

for generic value of m_χ. This in fact corresponds to $m_{T2}^{\max}$ for $m_\chi \geq m_{\tilde{\chi}_1^0}$:

$$m_{T2}^{\max}(m_\chi) = m_{\tilde{g}} - m_{\tilde{\chi}_1^0} + m_\chi \quad \text{for} \quad m_\chi \geq m_{\tilde{\chi}_1^0}, \tag{61}$$

which again gives $m_{T2}^{\max}(m_\chi = m_{\tilde{\chi}_1^0}) = m_{\tilde{g}}$.

By now, it should be clear that $m_{T2}^{\max}$ for $m_\chi < m_{\tilde{\chi}_1^0}$ has a different form from $m_{T2}^{\max}$ for $m_\chi > m_{\tilde{\chi}_1^0}$. As required, they should cross at $m_\chi = m_{\tilde{\chi}_1^0}$. *Thus, if the function $m_{T2}^{\max}(m_\chi)$ could be constructed from experimental data, one would be able to determine the true gluino and LSP masses separately.*

In order to see the experimental feasibility of measuring SUSY particle masses through the gluino stransverse mass at the LHC, we consider as an example a minimal anomaly mediated SUSY-breaking (mAMSB) scenario [34] with

$$m_{\tilde{g}} = 780.3 \text{ GeV}, \ m_{\tilde{\chi}_1^0} = 97.9 \text{ GeV}$$

and a few TeV masses for sfermions. We have generated a Monte Carlo sample of SUSY events for proton-proton collision at 14 TeV by PYTHIA [18] event generator. The event sample corresponds to 300 fb^{-1} integrated luminosity. We have also generated SM backgrounds such as $t\bar{t}, W/Z+jet, WW/WZ/ZZ$ and QCD events, with less equivalent luminosity. The generated events have been further processed with a modified version of fast detector simulation program PGS [19], which approximate an ATLAS- or CMS-like detector with reasonable efficiencies and fake rates.

The following event selection cuts are applied to have a clean signal sample for gluino stransverse mass;

1. At least 4 jets with $P_{T1,2,3,4} > 200, 150, 100, 50$ GeV
2. Missing transverse energy, $E_T^{miss} > 250$ GeV
3. Transverse sphericity, $S_T > 0.25$
4. No b-jets and no leptons

For each event, the four leading jets are used to calculate the gluino stransverse mass. The four jets are divided in two groups of dijets as follows. The highest momentum jet and the other jet which has the largest $|p_{jet}|\Delta R$ value with respect to the leading jet are chosen as two 'seed' jets for the division. Here, p_{jet} is the jet momentum and $\Delta R \equiv \sqrt{\Delta\phi^2 + \Delta\eta^2}$ *i.e.*, a separation in azimuthal angle and pseudorapidity plane. Each of the remaining two jets is associated to a seed jet, which makes the smallest opening angle. Then, each group of the dijets is considerd as orginated from the same mother particle (gluino).

Fig.12 shows the resulting distribution of the gluino stransverse mass for the trial LSP mass $m_\chi = 90$ GeV. The blue histogram corresponds to SM backgrounds. Fitting with a linear function with a linear background, we get the endpoint 778.0 ± 2.3 GeV. The measured edge values of $m_{T2}(\tilde{g})$, i.e. $m_{T2}^{\max}$, as a function of m_χ is shown in Fig.13. Blue and red lines denote the theoretical curves of (58) and (61), respectively, which have been obtained in this paper from the consideration of extreme momentum configurations. Fitting the data points to the curves (58) and (61), we obtain $m_{\tilde{g}} = 776.3 \pm 1.3$ GeV and $m_{\tilde{\chi}_1^0} = 97.3 \pm 1.7$ GeV, which are quite close to the true values, $m_{\tilde{g}} = 780.3$ GeV and $m_{\tilde{\chi}_1^0} = 97.9$ GeV. This demonstates that the gluino stransverse mass can be very useful for measuring the gluino and the LSP masses experimentally.

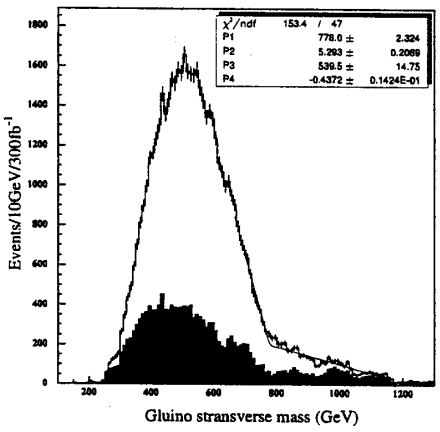

Figure 12: *The $m_{T2}(\tilde{g})$ distribution with $m_\chi = 90$ GeV for the benchmark point of mAMSB. Blue histogram is the SM background.*

Let us now consider the case that squark mass $m_{\tilde{q}}$ is smaller than gluino mass $m_{\tilde{g}}$. In such case, the following cascade decay is open;

$$\tilde{g} \to q\tilde{q} \to qq\tilde{\chi}_1^0. \tag{62}$$

In this case also, we consider two extreme momentum configurations which are similar to those considered for three body gluino decay, and construct the corresponding gluino stransverse

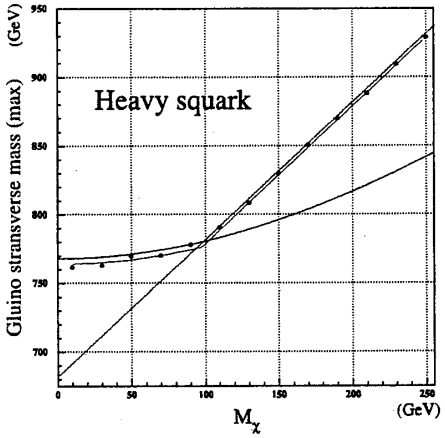

Figure 13: $m_{T2}^{\max}$ *as a function of the trial LSP mass* m_χ *for the benchmark point of mAMSB.*

masses. Here again, we assume gluinos are pair produced at rest and each gluino decays into a quark and a squark on the transverse plane with respect to the proton beam direction.

If the quark from squark decay is produced in the same direction to the first quark from gluino decay and the two sets of gluino decay products are parallel to each other, the transverse energies and transverse momenta of the qq systems are given by

$$\begin{aligned} E_T^{qq}(max) &\equiv E_T^{qq(1)} = E_T^{qq(2)} \\ &= |\mathbf{p}_T^{qq(1)}| = |\mathbf{p}_T^{qq(2)}| = \frac{m_{\tilde{g}}^2 - m_{\tilde{\chi}_1^0}^2}{2m_{\tilde{g}}}, \end{aligned} \tag{63}$$

just like Eq.(56) for the case of gluino three body decay, and we have $m_{qqT}^{(1)} = m_{qqT}^{(2)}$ for the transverse invariant masses of the qq systems and $|\mathbf{p}_T^{miss}| = 2E_T^{qq}(max)$ for the total observed missing transverse momentum. Then the same procedure to obtain the gluino stransverse mass for the first momentum configuration of the gluino three body decay is applied to the current case. It leads to $m_{T2}^{\max}$ which is same as Eq.(58):

$$\begin{aligned} m_{T2}^{\max}(m_\chi) &= \frac{m_{\tilde{g}}^2 - m_{\tilde{\chi}_1^0}^2}{2m_{\tilde{g}}} + \sqrt{\left(\frac{m_{\tilde{g}}^2 - m_{\tilde{\chi}_1^0}^2}{2m_{\tilde{g}}}\right)^2 + m_\chi^2} \\ &\quad \text{for} \quad m_\chi \leq m_{\tilde{\chi}_1^0}. \end{aligned} \tag{64}$$

Now we consider other extreme momentum configuration, in which the quarks from squark decays are produced in the opposite direction to the first quarks from gluino decays. In this case, the invariant transverse masses, transverse energies and transverse momenta of two qq systems are given by

$$\begin{aligned} m_{qqT}^{2(1)} &= m_{qqT}^{2(2)} = \frac{(m_{\tilde{g}}^2 - m_{\tilde{q}}^2)(m_{\tilde{q}}^2 - m_{\tilde{\chi}_1^0}^2)}{m_{\tilde{q}}^2}, \\ E_T^{qq(1)} &= E_T^{qq(2)} = \frac{m_{\tilde{g}}}{2}(1 - \frac{m_{\tilde{q}}^2}{m_{\tilde{g}}^2}) + \frac{m_{\tilde{g}}}{2}(1 - \frac{m_{\tilde{\chi}_1^0}^2}{m_{\tilde{q}}^2}), \\ |\mathbf{p}_T^{qq(1)} &= \mathbf{p}_T^{qq(2)}| = |\frac{m_{\tilde{g}}}{2}(1 - \frac{m_{\tilde{q}}^2}{m_{\tilde{g}}^2}) - \frac{m_{\tilde{g}}}{2}(1 - \frac{m_{\tilde{\chi}_1^0}^2}{m_{\tilde{q}}^2})|, \end{aligned}$$

respectively, and the total missing transverse momentum by $\mathbf{p}_T^{miss} = -2\ \mathbf{p}_T^{qq(1)}$. The two constraints, $m_T^{(1)} = m_T^{(2)}$ and $\mathbf{p}_T^{miss} = \mathbf{p}_T^{\chi(1)} + \mathbf{p}_T^{\chi(2)}$ for obtaining $m_{T2}(\tilde{g})$, then lead to $\mathbf{p}_T^{\chi(1)} = \mathbf{p}_T^{\chi(2)} = -\mathbf{p}_T^{qq(1)}$. Therefore, the gluino stransverse mass is expressed by

$$\begin{aligned} m_{T2}^2(\tilde{g}) &= m_{qqT}^{2(1)} + m_\chi^2 \\ &+ 2(E_T^{qq(1)}\sqrt{|\mathbf{p}_T^{qq(1)}|^2 + m_\chi^2} + |\mathbf{p}_T^{qq(1)}|^2). \end{aligned} \tag{65}$$

Again, one can show that this represents $m_{T2}^{\max}$ for $m_\chi \geq m_{\tilde{\chi}_1^0}$, yielding

$$\begin{aligned} m_{T2}^{\max} = &\left(\frac{m_{\tilde{g}}}{2}(1 - \frac{m_{\tilde{q}}^2}{m_{\tilde{g}}^2}) + \frac{m_{\tilde{g}}}{2}(1 - \frac{m_{\tilde{\chi}_1^0}^2}{m_{\tilde{q}}^2})\right) \\ &+\sqrt{\left(\frac{m_{\tilde{g}}}{2}(1 - \frac{m_{\tilde{q}}^2}{m_{\tilde{g}}^2}) - \frac{m_{\tilde{g}}}{2}(1 - \frac{m_{\tilde{\chi}_1^0}^2}{m_{\tilde{q}}^2})\right)^2 + m_\chi^2}. \end{aligned} \tag{66}$$

Note that the two functions (64) and (66) cross at $m_\chi = m_{\tilde{\chi}_1^0}$ for which $m_{T2}^{\max} = m_{\tilde{g}}$.

If one could construct (64) and (66) accurately enough from data, one would be able to determine all involved sparticle masses, i.e. $m_{\tilde{g}}, m_{\tilde{\chi}_1^0}$ and $m_{\tilde{q}}$. To see how feasible it is, we consider a parameter point of mirage mediation model [9, 10], providing the following sparticle masses;

$$m_{\tilde{g}} = 821.4 \text{ GeV},\ m_{\tilde{q}} = 694.0 \text{ GeV},\ m_{\tilde{\chi}_1^0} = 344.2 \text{ GeV}.$$

We have generated a Monte Carlo sample for this benchmark point of mirage mediation, corresponding to $100fb^{-1}$ integrated luminosity. After event selection cuts similar to the case of three body gluino decay, we obtain Fig.14 showing the distribution of $m_{T2}(\tilde{g})$ for the trial LSP mass $m_\chi = 350$ GeV. The edge value $m_{T2}^{\max}$ as a function of m_χ is shown in Fig.15. Fitting the data points to the curves (64) and (66), we obtain $m_{\tilde{g}} = 799.5 \pm 11.1$ GeV, $m_{\tilde{q}} = 678.2 \pm 7.0$ GeV and $m_{\tilde{\chi}_1^0} = 316.7 \pm 15.4$ GeV. Though the overall scale of the fitted values are well close to the true sparticle masses, the central values are somewhat lower than the true values. It is mainly due to a mild crossing of two curves, so that a precise determination of the $m_{T2}(\tilde{g})$ endpoint is crucial. The situation can be improved if we include information from *squark stransverse mass* for the process $pp \to \tilde{q}\tilde{q} \to q\tilde{\chi}_1^0 q\tilde{\chi}_1^0$, providing a relation between the edge value of the squark stransverse mass and the trial LSP mass:

$$m_{T2}^{\max}(\text{squark}) = \frac{m_{\tilde{q}}^2 - m_{\tilde{\chi}_1^0}^2}{2m_{\tilde{q}}} + \sqrt{\left(\frac{m_{\tilde{q}}^2 - m_{\tilde{\chi}_1^0}^2}{2m_{\tilde{q}}}\right)^2 + m_\chi^2}.$$

Including such information, we get $m_{\tilde{g}} = 803.4 \pm 6.0$ GeV and $m_{\tilde{\chi}_1^0} = 322.4 \pm 7.7$ GeV for the benchmark point. The discrepancy between the fitted mass values and the true mass values may still come from various systematic uncertainties such as the effects of event selection cuts.

To conclude, we have introduced the gluino stransverse mass, and shown that it can be used to determine the gluino and the lightest neutralino masses separately, and also the (1st and 2nd generation) squark masses if lighter than the gluino mass.

Acknowledgement

I thank the organisers of the Summer Institue 2007 for their hospitality and support.

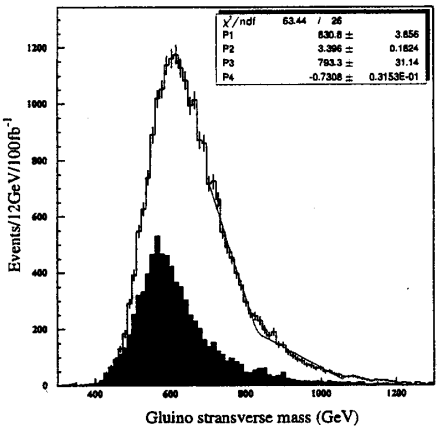

Figure 14: *The $m_{T2}(\tilde{g})$ distribution with $m_\chi = 350$ GeV for the benchmark point of mirage mediation.*

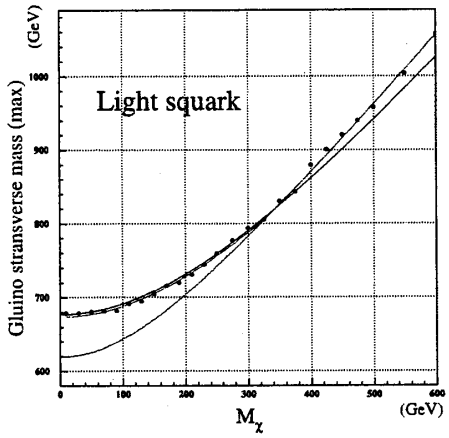

Figure 15: *$m_{T2}^{\max}$ as a function of the trial LSP mass m_χ for the benchmark point of mirage mediation.*

References

[1] ATLAS Technical Proposal, CERN-LHCC-94-43.

[2] CMS Physics Technical Design Report, CERN-LHCC-2006-021.

[3] H.P. Nilles, Phys. Rept. **110** (1984) 1; H.E. Haber and G.L. Kane, Phys. Rept. **117** (1985) 75; S.P. Martin, in Perspectives on Supersymmetry, ed. G.L. Kane, pp.1–98 [hep–ph/9709356].

[4] K. Choi and H. P. Nilles, JHEP **0704** (2007) 006.

[5] W.S. Cho, Y.G. Kim, K.Y. Lee, C.B. Park and Y.Shimizu, JHEP **0704**, 054 (2007) [arXiv:hep-ph/0703163].

[6] S.Y. Choi, K. Hagiwara, Y.G. Kim, K. Mawatari and P.M. Zerwas, Phys. Lett. **B 648** (2007) 207-212 [arXiv:hep-ph/0612237].

[7] W.S. Cho, K. Choi, Y.G. Kim, and C.B. Park, arXiv:0709.0288.

[8] S. Kachru, R. Kallosh, A. Linde and S. P. Trivedi, Phys. Rev. D **68**, 046005 (2003) [arXiv:hep-th/0301240].

[9] K. Choi, A. Falkowski, H. P. Nilles, M. Olechowski and S. Pokorski, JHEP **0411**, 076 (2004) [arXiv:hep-th/0411066]; K. Choi, A. Falkowski, H. P. Nilles and M. Olechowski, Nucl. Phys. **B718**, 113 (2005) [arXiv:hep-th/0503216].

[10] K. Choi, K. S. Jeong and K. i. Okumura, JHEP **0509**, 039 (2005) [arXiv:hep-ph/0504037].

[11] M. Endo, M. Yamaguchi and K. Yoshioka, Phys. Rev. D **72**, 015004 (2005) [arXiv:hep-ph/0504036]; A. Falkowski, O. Lebedev and Y. Mambrini, JHEP **0511**, 034 (2005) [arXiv:hep-ph/0507110]; K. Choi, K. S. Jeong, T. Kobayashi and K. i. Okumura, Phys. Lett. B **633**, 355 (2006) [arXiv:hep-ph/0508029]; R. Kitano and Y. Nomura, Phys. Lett. B **631**, 58 (2005) [arXiv:hep-ph/0509039]; O. Loaiza-Brito, J. Martin, H. P. Nilles and M. Ratz, hep-th/0509158; O. Lebedev, H. P. Nilles and M. Ratz, arXiv:hep-ph/0511320; R. Kitano and Y. Nomura, Phys. Rev. D **73**, 095004 (2006) [arXiv:hep-ph/0602096]; A. Pierce and J. Thaler, JHEP **0609**, 017 (2006) [arXiv:hep-ph/0604192]; K. Kawagoe and M. Nojiri, Phys. Rev. D **74**, 115011 (2006) [arXiv:hep-ph/0606104]; H. Baer, E. K. Park, X. Tata and T. T. Wang, JHEP **0608**, 041 (2006) [arXiv:hep-ph/0604253]; Phys. Lett. **B 641**, 447 (2006) [arXiv:hep-ph/0607085]; H. Baer, E. K. Park, X. Tata and T. T. Wang, hep-ph/0703024.

[12] K. Choi, K. Y. Lee, Y. Shimizu, Y. G. Kim and K.-i. Okumura, JCAP **0612**, 017 (2006) [arXiv:hep-ph/0609132].

[13] ATLAS Collaboration, Technical Design Report, CERN/LHCC/99–15 (1999); CMS Collaboration, Technical Proposal, CERN/LHCC/94–38 (1994); J.G. Branson, D. Denegri, I. Hinchliffe, F. Gianotti, F.E. Paige and P. Sphicas [ATLAS and CMS Collaborations], Eur. Phys. J. directC **4** (2002) N1.

[14] W. Beenakker, R. Hopker, M. Spira and P. M. Zerwas, Nucl. Phys. B **492**, 51 (1997) [arXiv:hep-ph/9610490].

[15] I. Hinchliffe, F. E. Paige, M. D. Shapiro, J. Soderqvist and W. Yao, Phys. Rev. D **55**, 5520 (1997) [arXiv:hep-ph/9610544]; H. Bachacou, I. Hinchliffe and F. E. Paige, Phys. Rev. D **62** (2000) 015009 [arXiv:hep-ph/9907518].

[16] G. Weiglein *et al.* [LHC/LC Study Group], Phys. Rept. **426** (2006) 47 [arXiv:hep-ph/0410364].

[17] WMAP Collaboration, D. N. Spergel *et al.* [arXiv:astro-ph/0603449]; Astrophys. J. Suppl. Ser. **148** (2003) 175.

[18] T. Sjostrand, P. Eden, C. Friberg, L. Lonnblad, G. Miu, S. Mrenna and E. Norrbin, Computer Physics Commun. 135 (2001) 238; T. Sjostrand, S. Mrenna and P. Skands, LU TP 06-13, FERMILAB-PUB-06-052-CD-T [hep-ph/0603175].

[19] http://www.physics.ucdavis.edu/ conway/research/software/pgs/pgs4-general.htm

[20] M. Drees, Y.G. Kim, M.M. Nojiri, D. Toya, K. Hasuko and T. Kobayashi, Phys. Rev. **D 63** (2001) 035008 [arXiv:hep-ph/0007202].

[21] C. G. Lester and D. J. Summers, Phys. Lett. **B 463** (1999) 99-103; A. Barr, C. Lester, and P. Stephens, J. Phys. **G 29** (2003) 2343.

[22] B. C. Allanach *et al.*, "The Snowmass points and slopes: Benchmarks for SUSY searches," Eur. Phys. J. C **25** (2002) 113 [arXiv:hep-ph/0202233].

[23] A. J. Barr, "Using lepton charge asymmetry to investigate the spin of supersymmetric Phys. Lett. B **596**, 205 (2004) [arXiv:hep-ph/0405052].

[24] T. Goto, K. Kawagoe and M. M. Nojiri, "Study of the slepton non-universality at the CERN Large Hadron Collider," Phys. Rev. D **70** (2004) 075016 [Erratum-ibid. D **71** (2005) 059902] [arXiv:hep-ph/0406317].

[25] J. M. Smillie and B. R. Webber, "Distinguishing spins in supersymmetric and universal extra dimension models at the Large Hadron Collider," JHEP **0510** (2005) 069 [arXiv:hep-ph/0507170]; C. Athanasiou, C. G. Lester, J. M. Smillie and B. R. Webber, "Distinguishing spins in decay chains at the Large Hadron Collider," JHEP **0608** (2006) 055 [arXiv:hep-ph/0605286].

[26] L. T. Wang and I. Yavin, "Spin measurements in cascade decays at the LHC," arXiv:hep-ph/0605296.

[27] M. M. Nojiri, Phys. Rev. D **51** (1995) 6281 [arXiv:hep-ph/9412374]; M. M. Nojiri, K. Fujii and T. Tsukamoto, Phys. Rev. D **54** (1996) 6756 [arXiv:hep-ph/9606370].

[28] B. K. Bullock, K. Hagiwara and A. D. Martin, "Tau Polarization And Its Correlations As A Probe Of New Physics," Nucl. Phys. B **395** (1993) 499.

[29] S. Y. Choi, J. Kalinowski, G. A. Moortgat-Pick and P. M. Zerwas, "Analysis of the neutralino system in supersymmetric theories," Eur. Phys. J. C **22** (2001) 563 [Addendum-ibid. C **23** (2002) 769] [arXiv:hep-ph/0108117].

[30] E. Boos, H. U. Martyn, G. A. Moortgat-Pick, M. Sachwitz, A. Sherstnev and P. M. Zerwas, "Polarisation in sfermion decays: Determining tan(beta) and trilinear couplings," Eur. Phys. J. C **30**, 395 (2003) [arXiv:hep-ph/0303110].

[31] T. Appelquist, H. C. Cheng and B. A. Dobrescu, "Bounds on universal extra dimensions," Phys. Rev. D **64**, 035002 (2001) [arXiv:hep-ph/0012100].

[32] H. C. Cheng, K. T. Matchev and M. Schmaltz, "Radiative corrections to Kaluza-Klein masses," Phys. Rev. D **66** (2002) 036005 [arXiv:hep-ph/0204342].

[33] D. J. Mangeol and U. Goerlach, "Search for $\tilde{\chi}_2^0$ decays to $\tilde{\tau}\tau$ and SUSY mass spectrum measurment using di-τ final states", CMS note 2006/096.

[34] L. Randall and R. Sundrum, Nucl. Phys. **B 557** (1999) 79 [hep-th/9810155]; G. F. Giudice, M. A. Luty, H. Murayama and R. Rattazzi, JHEP **12** (1998) 027 [hep-ph/9810442].